pubs.acs.org/JPCC

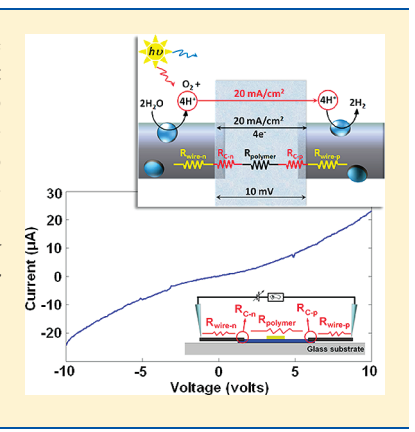
# Characterization of the Electrical Properties of Individual p-Si Microwire/Polymer/n-Si Microwire Assemblies

Iman Yahyaie, Kevin McEleney, Michael G. Walter, Derek R. Oliver, Douglas J. Thomson, Michael S. Freund, and Nathan S. Lewis

<sup>†</sup>Department of Electrical and Computer Engineering, <sup>‡</sup>Department of Chemistry, University of Manitoba, Winnipeg, Manitoba, Canada <sup>§</sup>Beckman Institute and Kavli Nanoscience Institute, Division of Chemistry and Chemical Engineering, M/C 127-72, 210 Noyes Laboratory, California Institute of Technology, Pasadena, California 91125, United States



**ABSTRACT:** The electrical properties of individual p- and n-type silicon microwires have been investigated using a direct contact formation technique, in which an Ohmic contact between the tungsten probe and microwire was produced by applying mechanical force to the probe/microwire junction. This method alleviated the need for lithography or a high-temperature process to form a metal/Si ohmic contact. The technique was also used to characterize the Si microwire/conducting polymer junctions in a single cell of a membrane-supported bilayer Si microwire structure that is of interest for the direct production of fuels from sunlight. The data indicate that the combination of PEDOT—PSS—Nafion and highly doped Si microwires is suitable, from an electrical resistance perspective, to be used in a solar fuels generation device.



#### 1. INTRODUCTION

A membrane-bridged bilayer microwire structure is an interesting conceptual approach to the production of fuels from sunlight. This integrated system would ideally use water and sunlight as inputs, and would generate  $H_2(g)$  and  $O_2(g)$  as outputs. This type of solar water-splitting device would consist of four main components (Figure 1): arrays of semiconducting microwires, to effectively absorb sunlight and provide sufficient photovoltage to produce fuel at high energy conversion efficiency; a two-electron catalyst to facilitate the reduction of protons to  $H_2$  at the cathode; a four-electron catalyst to facilitate the oxidation of water to  $O_2$  at the anode; and a membrane that separates the products for safety and efficiency purposes, provides a suitable electrical connection between the microwires, and allows for neutralization of the pH gradient that would otherwise be produced during fuel production.  $^{4,5}$ 

The membrane-supported assembly, consisting of semiconducting microwires supported in a conducting polymer film, will be a chemically complex structure with critical features on and below the micrometer scale. Silicon microwire arrays are currently used in a wide range of applications from solar cells<sup>6–9</sup> to organic, <sup>10</sup> liquid junction, <sup>11,12</sup> and inorganic solid-state <sup>7</sup> devices. In conjunction with suitable electrocatalysts, such structures offer an interesting platform to develop a photocathode for H<sub>2</sub> production from water. <sup>13</sup> A variety of electrical parameters, including the Si microwire resistivity, the doping distribution, and the total series resistances in the microwire/conducting polymer system,

will have to be optimized to meet the performance specifications for the proposed device. The nature of the electrical junctions between the doped silicon microwires and different candidate conducting polymers will be an important factor in the proper function of the final water-splitting device (Figure 1).

A straightforward method has recently been reported for characterizing the electrical properties of p-type Si microwires as well as the junction between Si microwires and conducting polymers. This work presents the application of this technique to n-type silicon microwires in contact with a prototypical conducting polymer. We also report DC electrical measurements across a single unit of the proposed solar fuels generation device, obtained by measuring the full-system electrical conductivity in a structure that consisted of a single n-Si microwire contacted to a conducting polymer that in turn was also in contact with a single p-Si microwire.

## 2. EXPERIMENTAL METHODS

**2.1. Si Microwires.** Si microwires were grown using the vapor—liquid—solid chemical vapor deposition (CVD) process. <sup>11,15,16</sup> The single crystalline Si microwires were  $60-120~\mu m$  in length and  $\sim 1.5-2.0~\mu m$  in diameter. The Si microwires were doped

Received: September 14, 2011 Revised: October 27, 2011 Published: November 04, 2011

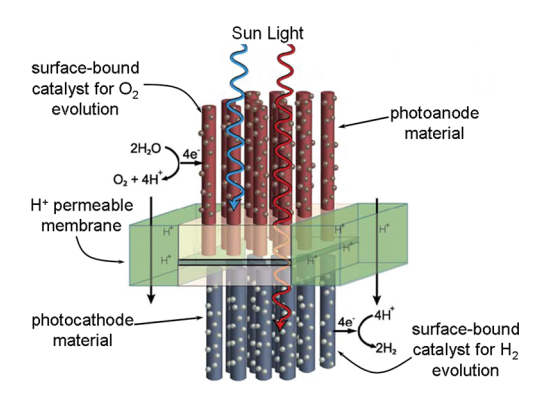


**Figure 1.** Schematic diagram of the proposed solar fuel generation device structure. Reprinted with permission from ref 3. Copyright 2008 California Institute of Technology.

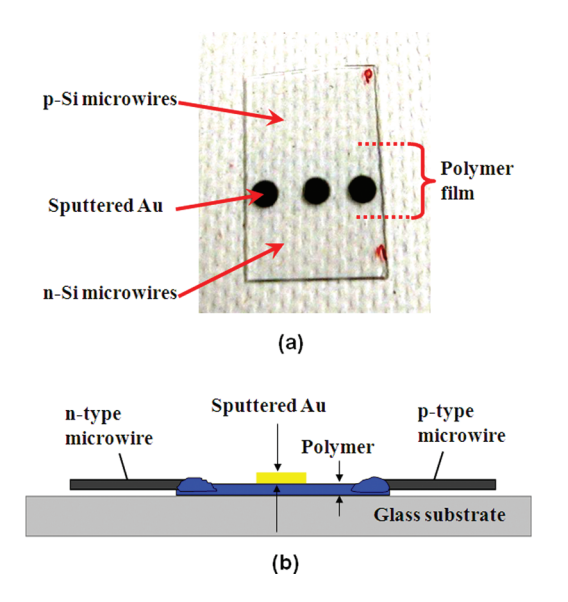


**Figure 2.** (a) Photograph of the test structure; (b) schematic diagram of the system. The PEDOT-PSS-Nafion strip was spin-coated onto a glass substrate. The film dimensions were  $\sim$ 1 cm by 2.5 cm, and the film thickness was  $\sim$ 200 nm. p- and n-Si microwires were aligned at the polymer/glass border as shown, and Au contacts (32 nm thick) were sputtered onto the polymer membrane, to complete the test structure; 2–5  $\mu$ m of the wire was embedded into the polymer.

with boron (p-type) and phosphorus (n-type) up to doping levels of  $10^{17}-10^{18}$  cm  $^{-3}$ . Any residual metallic growth catalyst at the top of each microwire (and some small amounts on the sides) from the vapor—liquid—solid (VLS) growth process was removed using a two-step etching procedure (Supporting Information). Prior to the measurements, the native oxide, as well as any oxide that may have formed during the growth catalyst removal process, was removed by etching the Si microwires in buffered HF(aq). The time interval between the native oxide removal process and the measurements was kept as short as possible (typically <15 min).

**2.2. Conducting Polymer Films.** Solutions of a candidate conducting polymer, polyethylenedioxythiophene/polystyrene sulfonate/Nafion (PEDOT-PSS-Nafion)<sup>17</sup> with 12 wt.% PEDOT-PSS, were prepared according to established procedures (Supporting Information). Thick conducting polymer

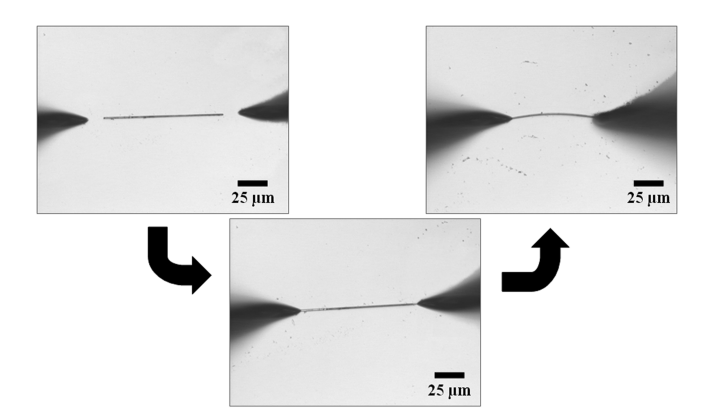


**Figure 3.** Use of tungsten probes to mechanically manipulate silicon microwires. The force required to bend a microwire greatly exceeded the force that was applied during the electrical measurements.

layers (150 and 200 nm) were deposited by spin-coating a solution of polymer onto a glass substrate that contained prepositioned Parafilm masks on the left and right sides of one surface of the substrate. Ohmic contacts were then formed to the conducting polymer films by sputtering 32 nm thick pads of gold directly onto the polymer. Following the removal of the Parafilm mask, p-type and n-type Si microwires were separately deposited onto the exposed glass substrate. Single microwires were then aligned with tungsten probes, and the wires were positioned perpendicular to the border between the conducting polymer and the glass substrate with 2–5  $\mu$ m of the wire in contact with the polymer. This structure was used as a template of a single unit of the proposed solar fuels generation device (Figure 2).

**2.3. Instruments.** Current vs voltage (I-V) measurements were performed in a standard probe station using an Agilent 4155c semiconductor parameter analyzer. Standard tungsten probes (with a diameter of  $\sim 1~\mu \text{m}$ ), used in the I-V measurements, were etched for  $\sim 30~\text{s}$  in 2.0 M KOH(aq) immediately before the experiments to remove the tungsten native oxide and to improve the quality of the contacts. An Edwards s150b sputter coater was used to sputter Au pads onto the polymers. A Fogale Photomap 3D optical profilometer and a KLA Tencore AS-500 Alpha-Step were used for measurements of the polymer film thickness. X-ray photoelectron spectroscopic (XPS) analysis was performed using a Kratos Axis Ultra DLD instrument.

## 3. RESULTS AND DISCUSSION

**3.1. Single Microwire Measurements.** Thermal evaporation of contact metals has been used to form Ohmic contacts to individual Si microwires. <sup>18–20</sup> Despite the high-yield of this procedure, this lithographic, high-temperature process is only applicable to a certain range of microwire diameters and is not compatible with many microwire/polymer structures due to the complexity of interactions between polymers, photoresists, and the etchant solutions used during lithographic processes. In this work, the electrical properties of single Si microwires and of Si microwire/polymer junctions were simply and readily characterized by the use of tungsten (W) probes to make direct, reliable contacts to the Si microwires. The tungsten probes additionally allowed for mechanical manipulation of the microwires (Figure 3), as well as for the formation of electrical contacts to the individual microwires.

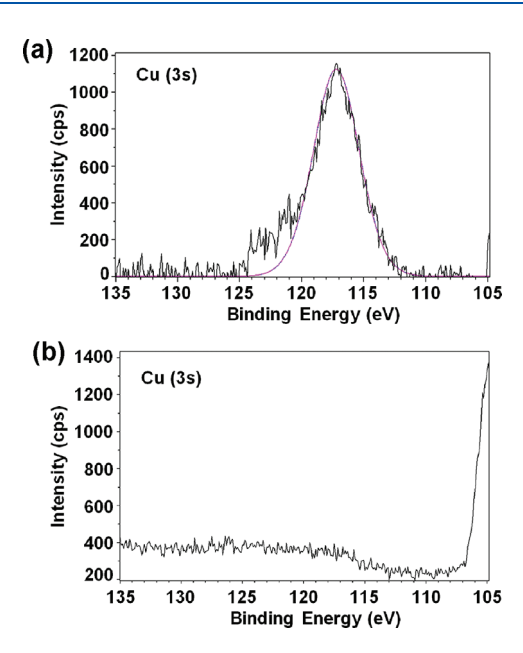
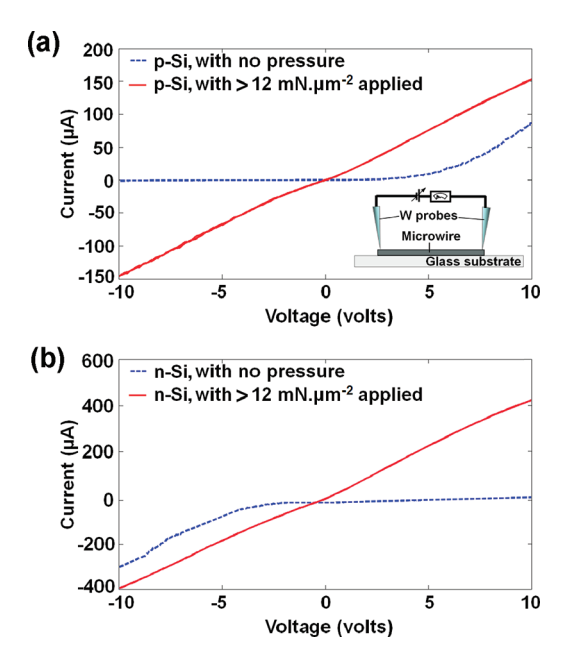


Figure 4. XPS data (a) before and (b) after the catalyst removal procedure, to confirm the removal of Cu from Si microwires grown from a Cu VLS catalyst.

After the process steps designed to remove the growth catalyst and the native oxide (vide supra, section 2.1), XPS confirmed that the growth catalyst had been eliminated (Figure 4). Current—voltage (I-V) measurements were then performed at various probe separations along the microwires, to show that the measurements were consistent with expectations for variation in the positions of the probes. These data allowed for determination of the probe/microwire contact resistance and for characterization of the uniformity of the doping concentration along individual microwires.

The mechanism of contact formation between the W-probes and the Si microwires in these measurements differs from many conventional methods for producing ohmic contacts  $^{18-20}$  because the tungsten probes were applied directly to the Si microwire without the need for high temperature treatment or lithography.  $^{14}$  One explanation for the observed electrical behavior of the W/Si wire contacts is the effect of local pressure at the point of contact. The resistivity of silicon has been reported to vary as a function of pressure.  $^{21,22}$  The application of  $\sim \! 112,\! 000$  kg  $\cdot \! \, \mathrm{cm}^{-2}$ , i.e.,  $\sim \! 11$  mN  $\cdot \! \, \mu \mathrm{m}^{-2}$ , to planar Si samples has been reported to change the contact character from a Schottky contact to an ohmic contact.  $^{23}$ 

The force exerted on the microwires by the tungsten probes was measured to stabilize at a maximum value of  $\sim$ 37 mN (Supporting Information). Assuming a maximum circular contact diameter of 2  $\mu$ m (based on the maximum diameter of the microwires), the local mechanical pressure at the point of contact was thus >12 mN· $\mu$ m<sup>-2</sup>. The transition in electronic character of the contact as a function of pressure was observed by alternately increasing and decreasing the pressure on the microwires. Figure 5 (dashed line) shows the measured I-V response for individual p- and n-type microwires, with >12 mN· $\mu$ m<sup>-2</sup> of mechanical pressure applied to the contact between the probe that was fixed at one end of the microwire, with the second probe loosely connected to the other end of the microwire (with no additional force). The solid line in Figure 5 shows the change in the I-V profile that resulted from the application of >12 mN· $\mu$ m<sup>-2</sup> of



**Figure 5.** Local phase transition in response to mechanical pressure at the contact areas. A 100  $\mu$ m long (a) p-Si microwire and (b) n-Si microwire was investigated with the first probe fixed at one end of the microwire with >12 mN· $\mu$ m<sup>-2</sup> of local pressure applied, while the second probe touched the other end with almost no applied force (blue curve) or with the same amount of force applied to both probes (red curve). As the pressure increased, the phase transition occurred, changing the nonlinear I-V behavior to that expected for an ohmic contact. The fixed probe was connected to the Common/Frame Ground terminal of the parameter analyzer.

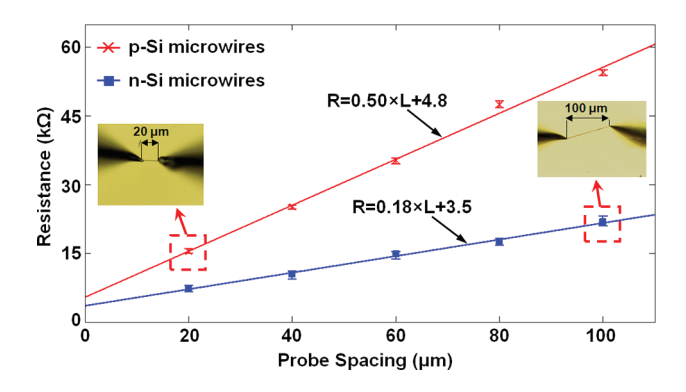


Figure 6. Contact resistance measurements for p- and n-type Si microwires with  $\sim 1.5~\mu m$  diameter. Seven independent measurements were carried out for each selected point across the length of the microwire. The data set from one pair of microwires are shown, these results were verified by repeating the experiment with other microwires of different doping type, different doping concentration, and originating from different fabrication batches.

mechanical pressure via the second probe. This observation was reversible for both types of microwires and could be readily repeated by increasing or decreasing the force applied to the probes.

Figure 6 depicts the resistance vs probe separation data obtained for p-type and n-type Si microwires. Each data point is the average of seven independent measurements in which the probe was completely disconnected from the microwire before the contact

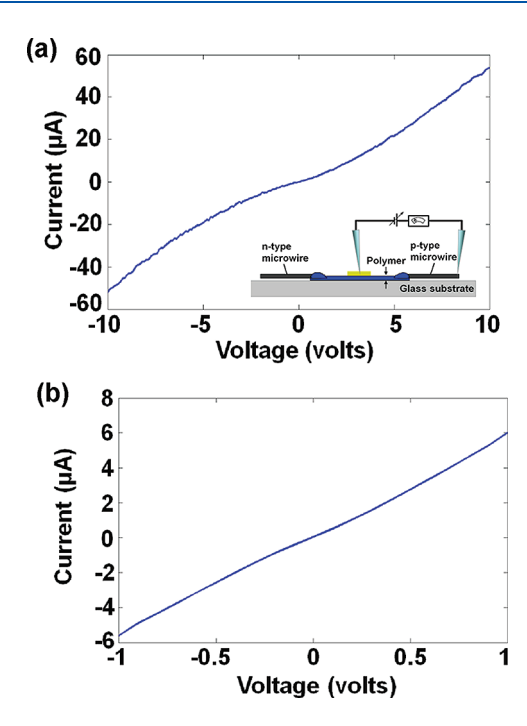


Figure 7. Current—voltage data for a 100 μm long p-type silicon microwire with a diameter of  $\sim$  1.5 μm aligned at the PEDOT—PSS—Nafion/ glass border (figure inset) for different ranges of applied bias voltages: (a) large-bias regime, -10 V to +10 V; and (b) small-bias regime, -1 V to +1 V. The total series resistance of the system in the large-bias regime was  $\sim$ 150 k $\Omega$  but increased to  $\sim$ 172 k $\Omega$  in the small-bias regime.

for the next measurement was made. The data thus demonstrate the reliability and reproducibility of the contacts to both p- and n-type microwires. The resistance per unit length was constant for all of the measurements, at values of 0.50 k $\Omega \cdot \mu m^{-1}$  for the p-type and 0.18 k $\Omega \cdot \mu \text{m}^{-1}$  for the n-type Si microwires. The contact resistance was calculated by performing a linear fit to the resistance versus probe separation data, in conjunction with the evaluation of the intercept of such a plot (Figure 6). The calculated contact resistance values were reasonably similar for both types of Si microwires, which is consistent with expectations based on a pressure-induced phase transition forming the measured probe-wire contact. Although the calculations showed that the contact resistance was a negligible contribution to the total measured resistance, the contact resistance was subtracted prior to calculating the resistivity of the microwires and, in turn, prior to the estimation of the doping concentration of the microwires.

By using the contact resistance data, the doping concentration of the microwires was estimated to be  $10^{17}-10^{18}~{\rm cm}^{-3}$ . This is within the expected range of doping concentrations based on the conditions used to grow the Si microwires. <sup>18,24</sup> No variation in the resistance measurements was observed between different regions of the microwires or different microwires, indicating that the p- and n-type doping concentration was uniform over the length scales considered. The difference in the value of the resistance per length between the two types of microwires is in good accord with the difference in the mobility values of the majority carriers in p- and n-type microwires at these doping concentrations. <sup>25</sup>

**3.2.** Microwire/Conducting Polymer Junction Measurements. Figure 2 shows the test structure that was used to investigate the electrical behavior of p-type Si and n-type Si

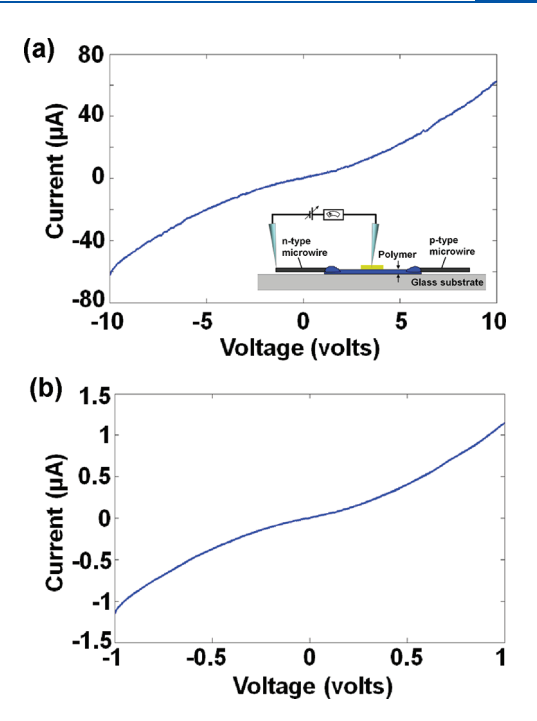


Figure 8. Current—voltage data for a 100  $\mu m$  long n-type Si microwire with a diameter of  $\sim 1.5 \, \mu m$  aligned at the PEDOT—PSS—Nafion/glass border (figure inset) for different ranges of applied bias voltages: (a) large-bias regime,  $-10 \, V$  to  $+10 \, V$ ; and (b) small-bias regime,  $-1 \, V$  to  $+1 \, V$ . The total series resistance of the system in the large-bias regime was  $\sim 115 \, k\Omega$ , and increased to  $\sim 870 \, k\Omega$  in the small-bias regime.

microwire/polymer junctions. Using the tungsten probes, the microwires aligned on the polymer films were covered with a small amount of polymer to ensure electrical contact between the polymer and the  $2-5~\mu m$  of the microwire in contact with the polymer. Even though the eventual embedding depth of the microwires in the polymer membrane has not been finalized, this configuration more closely resembled the eventual envisioned device structure (Figure 1) than did a configuration in which a microwire was physically on top of a planar polymer film layer. Scanning electron microscopy (SEM) and Auger electron spectroscopy (AES) imaging indicated the presence of an intimate contact between the polymer and microwire, as well as a sharp border between the polymer and the substrate.  $^{14}$ 

The three main junctions in the final measurement system were therefore: (a) the sputtered gold/polymer junction; (b) the tungsten probe/microwire junction; and (c) the microwire/polymer junction in between the other two junctions. The sputtered gold/polymer junction exhibited well-defined ohmic characteristics (Supporting Information). The contact resistance of the tungsten probe/microwire junction (section 3.1) was negligible when compared to the resistance of other parts of the system.

In one set of measurements (Figure 2), the contributions from each type of microwire and their junctions with the conducting polymer were individually investigated. The experiments were performed by recording the current that passed through the system for different applied voltages, with one tungsten probe in contact with the microwire, while the other probe was placed on the gold contact (insets of Figures 7a and 8a). The I-V data for p- and n-type microwires aligned at the PEDOT-PSS-Nafion/glass border are shown in Figures 7 and 8, respectively. At low voltages, the I-V behavior of the junction between the microwires

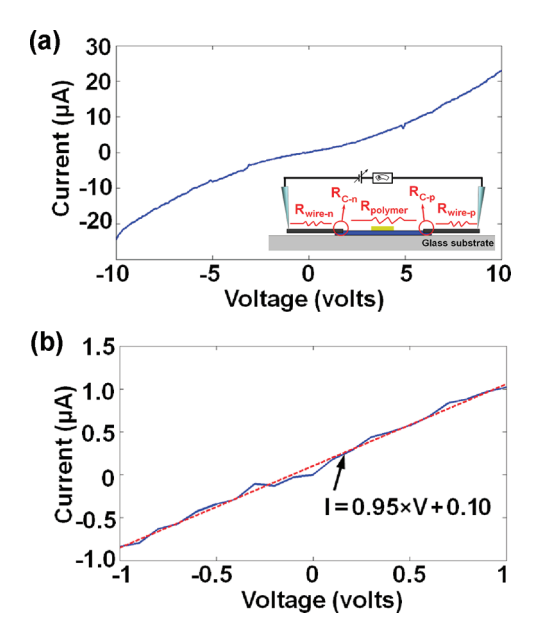


Figure 9. Complete unit of the proposed solar fuel generator device, including two 100 μm long n-type and p-type Si microwires with a diameter of  $\sim$ 1.5 μm, aligned at the PEDOT–PSS–Nafion/glass border (figure inset). Current–voltage data measured for different ranges of applied bias voltages: (a) large-bias regime, -10~V to +10 V; and (b) small-bias regime, -1~V to +1 V. The total series resistance of the system in the large-bias regime was  $\sim$ 250 k $\Omega$  and increased to  $\sim$ 1 M $\Omega$  in the small-bias regime.

and polymer films was nonlinear, likely due to tunneling through an oxide layer on the surface of the microwires, in accord with prior measurements on oxide-coated Si microwire devices. Although the Si microwires were etched immediately prior to the measurements, a thin layer of native oxide presumably formed on the surface of the Si because the alignment of the microwires at the polymer/glass interface was conducted in an air ambient. Hence, in addition to the measurements at small-bias (closer to the expected working regime of the solar fuels generation device), the total resistance values for the system were also measured at higher bias voltages, where nonlinear behavior was not dominant, and the I-V profile appeared purely resistive. The large-bias measurements thus yield a lower bound for values of the DC resistance of the system.

In each case, the total series resistance included contributions from the conducting polymer resistance,  $R_{\rm polymer}$ , the microwire/polymer contact resistance,  $R_{\rm C}$  (denoted as  $R_{\rm C-p}$  for p-type and  $R_{\rm C-n}$  for n-type microwires), and the microwire resistance,  $R_{\rm wire}$  (denoted as  $R_{\rm p-wire}$  for p-type and  $R_{\rm n-wire}$  for n-type microwires). The microwire/polymer contact resistance ( $R_{\rm C}$ ) was then calculated from the expression

$$R_{\text{total}} = R_{\text{polymer}} + R_{\text{wire}} + R_{\text{C}}$$

where,  $R_{\rm total}$  is the total measured resistance of the microwire/polymer system.  $R_{\rm polymer}$  was calculated from four-point probe measurements. The  $R_{\rm C-p}$  and  $R_{\rm C-n}$  values were extracted from these independent measurements, and the total series resistance across a single unit of the membrane-bridged device was then approximated by adding these values to the values of  $R_{\rm p-wire}$ ,  $R_{\rm n-wire}$  and  $R_{\rm polymer}$ .

The results of these calculations were also compared to the results of a measurement on a complete structure (Figure 9) in

Table 1. Measured and Calculated Resistances in k $\Omega$  ( $\pm 1\%$ ) of the Si Microwires of Lengths and Diameters of 100 and 1.5  $\mu$ m, Respectively<sup>a</sup>

$R_{\mathrm{meas}}\left(\mathrm{k}\Omega\right)$	$R_{ m p-wire}$	$R_{\text{n-wire}}$	$R_{\text{C-p}}$	$R_{C-n}$	$R_{ m polymer}$	$R_{\text{total}}$
large-bias	50	18	~100	~93	2	~263
small-bias	50	18	~120	~850	2	~1040
$^{a}R_{\mathrm{polymer}}$ is the resistance of the PEDOT-PSS-Nafion film.						

which one tungsten probe was placed on the n-type microwire, the second probe contacted the p-type wire, and a test current was passed through the entire structure.

Table 1 summarizes the measured resistances for both small-and large-bias regimes and shows that the measured value of  $R_{\text{C-p}}$  in the small-bias regime was 20 k $\Omega$  larger than the value recorded at the large-bias. This behavior can be ascribed to the presence of a thin native oxide layer on the microwire. However, the 8-fold increase in the value of  $R_{\text{C-n}}$  in the small-bias regime reflected both the presence of a native oxide layer on the microwires and the Fermi level mismatch between the n-type microwires and PEDOT-PSS-Nafion film (with p-type characteristics).  $^{28,29}$  The results from both the small- and large-bias measurements were in reasonable agreement (Table 1).

In estimating the performance of these microwire/polymer combinations in the proposed solar fuel generation device, the design parameters suggest that a maximum current of  $\sim$ 20.9 nA will flow along an individual 2  $\mu$ m diameter Si microwire through the junction to the polymer film.<sup>14</sup> Also, for this design, the maximum acceptable voltage drop across the microwire/ membrane junction is ~10 mV; thus, the total resistance needs to be <480 k $\Omega$ . The calculated resistance values at large-bias voltages  $(\pm 10 \text{ V})$  indicate that PEDOT-PSS-Nafion with silicon microwires would provide a viable candidate system for the construction of a membrane-bridged solar fuel generation device. However, at bias voltages close to the actual expected working conditions ( $\pm 10 \,\mathrm{mV}$ ), higher resistances were observed, indicating that the microwire surface treatment (e.g., native oxide removal) had a significant impact on the electrical properties of the Si/polymer junctions. The total resistance is also sensitive to the contact area between the silicon microwires and conducting polymer films. If in the final design for the artificial photosynthesis system the silicon microwires are embedded more than the  $2-5 \mu m$  (as presented here), then the values of  $R_{C-p}$  and  $R_{C-n}$ would correspondingly decrease. This would reduce the difference between the reported  $R_{\text{total}}$  and the design specifications referred to above. Regardless, improvements in IR losses at the low current levels (by up to a factor of  $\sim$ 2), for n-Si microwire/ PEDOT-PSS contacts, are desirable to satisfy the design requirements for the envisioned solar fuels generation device.

## 4. CONCLUSIONS

An approach to electrical contact formation, using tungsten probes, was successfully applied to n-type Si microwires. The method was used to characterize an individual unit of a proposed solar fuel generation device. The advantage of the method is that the contact was formed only by applying force to the probe—microwire junction, alleviating the need for lithography and for a high-temperature process step to form a metal/Si ohmic contact. The local pressure in the immediate contact area of the Si microwire resulted in a local phase transition, generating a stable and reproducible ohmic contact. The data indicate that the

PEDOT-PSS-Nafion/microwire system would provide a suitable combination, from an electrical resistance perspective, to be used in a solar fuels generation device.

## ■ ASSOCIATED CONTENT

**Supporting Information.** Metallic catalyst removal procedure, conductive polymer film preparation, microwire/polymer junction formation, and quantifying the applied mechanical force on the single silicon microwires. This material is available free of charge via the Internet at http://pubs.acs.org.

## AUTHOR INFORMATION

## **Corresponding Author**

\* Tel: +1-204-474-9563. E-mail: derek\_oliver@umanitoba.ca.

## **Present Address**

Department of Chemistry, University of North Carolina at Charlotte, Charlotte, North Carolina 28223, United States.

#### ACKNOWLEDGMENT

Financial support is gratefully acknowledged from the following: the Natural Sciences and Engineering Research Council (NSERC) of Canada, the Canada Foundation for Innovation (CFI), the Manitoba Research and Innovation Fund, and the University of Manitoba. The work reported made use of the Manitoba Materials and Surface Characterization Facility. This work was supported by a National Science Foundation (NSF) Center for Chemical Innovation (CCI) Powering the Planet (grants CHE-0802907, CHE-0947829, and NSF-ACCF), support for M.G.W. (CHE-0937048) by the Stanford Global Climate and Energy Program, and by Toyota, and made use of the Molecular Materials Research Center of the Beckman Institute at Caltech and the Kavli Nanoscience Institute at Caltech. This research was undertaken, in part, thanks to funding from the Canada Research Chairs Program.

## ■ REFERENCES

- (1) Gray, H. B. Powering the Planet with Solar Fuel. *Nat. Chem.* **2009**, *1* (1), 7–7.
- (2) Walter, M. G.; Warren, E. L.; McKone, J. R.; Boettcher, S. W.; Mi, Q. X.; Santori, E. A.; Lewis, N. S. Solar Water Splitting Cells. *Chem. Rev.* **2010**, *110* (11), 6446–6473.
- (3) California Institute of Technology. CCI Powering the Planet: An NSF Center for Chemical Innovation. http://ccisolar.caltech.edu (accessed Aug 2011).
- (4) Hu, X.; Brunschwig, B. S.; Peters, J. C. Electrocatalytic Hydrogen Evolution at Low Overpotentials by Cobalt Macrocyclic Glyoxime and Tetraimine Complexes. *J. Am. Chem. Soc.* **2007**, *129* (29), 8988–8998.
- (5) Jiao, F.; Frei, H. Nanostructured Cobalt Oxide Clusters in Mesoporous Silica as Efficient Oxygen-Evolving Catalysts. *Angew. Chem., Int. Ed.* **2009**, 48 (10), 1841–1844.
- (6) Tsakalakos, L.; Balch, J.; Fronheiser, J.; Shih, M. Y.; LeBoeuf, S. F.; Pietrzykowski, M.; Codella, P. J.; Korevaar, B. A.; Sulima, O.; Rand, J.; Davuluru, A.; Rapol, U. Strong Broadband Optical Absorption in Silicon Nanowire Films. *J. Nanophotonics* **2007**, *1*, 1355/2–1355/10.
- (7) Peng, K. Q.; Xu, Y.; Wu, Y.; Yan, Y. J.; Lee, S. T.; Zhu, J. Aligned Single-Crystalline Si Nanowire Arrays for Photovoltaic Applications. *Small* **2005**, *1* (11), 1062–1067.
- (8) Hu, L.; Chen, G. Analysis of Optical Absorption in Silicon Nanowire Arrays for Photovoltaic Applications. *Nano Lett.* **2007**, *7* (11), 3249–3252.

- (9) Tian, B. Z.; Zheng, X. L.; Kempa, T. J.; Fang, Y.; Yu, N. F.; Yu, G. H.; Huang, J. L.; Lieber, C. M. Coaxial Silicon Nanowires as Solar Cells and Nanoelectronic Power Sources. *Nature* **2007**, *449*, 885–889.
- (10) Huynh, W. U.; Dittmer, J. J.; Alivisatos, A. P. Hybrid Nanorod-Polymer Solar Cells. *Science* **2002**, 295, 2425–2427.
- (11) Maiolo, J. R.; Kayes, B. M.; Filler, M. A.; Putnam, M. C.; Kelzenberg, M. D.; Atwater, H. A.; Lewis, N. S. High Aspect Ratio Silicon Wire Array Photoelectrochemical Cells. *J. Am. Chem. Soc.* **2007**, 129 (41), 12346–12347.
- (12) Goodey, A. P.; Eichfeld, S. M.; Lew, K. K.; Redwing, J. M.; Mallouk, T. E. Silicon Nanowire Array Photoelectrochemical Cells. *J. Am. Chem. Soc.* **2007**, 129 (41), 12344–12345.
- (13) Boettcher, S. W.; Warren, E. L.; Putnam, M. C.; Santori, E. A.; Turner-Evans, D.; Kelzenberg, M. D.; Walter, M. G.; McKone, J. R.; Brunschwig, B. S.; Atwater, H. A.; Lewis, N. S. Photoelectrochemical Hydrogen Evolution Using Si Microwire Arrays. *J. Am. Chem. Soc.* **2011**, 133 (5), 1216–1219.
- (14) Yahyaie, I.; McEleney, K.; Walter, M.; Oliver, D. R.; Thomson, D. J.; Freund, M. S.; Lewis, N. S. Electrical Characterization of Si Microwires and of Si Microwire/Conducting Polymer Composite Junctions. J. Phys. Chem. Lett. 2011, 2 (6), 675–680.
- (15) Kayes, B. M.; Filler, M. A.; Putnam, M. C.; Kelzenberg, M. D.; Lewis, N. S.; Atwater, H. A. Growth of Vertically Aligned Si Wire Arrays over Large Areas (> 1 cm<sup>2</sup>) with Au and Cu Catalysts. *Appl. Phys. Lett.* **2007**, *91* (10), 103110–110113.
- (16) Wagner, R. S.; Ellis, W. C. Vapor-Liquid-Solid Mechanism of Single Crystal Growth. *Appl. Phys. Lett.* **1964**, 4 (5), 89–90.
- (17) McFarlane, S. L.; Day, B. A.; McEleney, K.; Freund, M. S.; Lewis, N. S. Designing Electronic/Ionic Conducting Membranes for Artificial Photosynthesis. *Energy Environ. Sci.* **2011**, 4 (5), 1700–1703.
- (18) Kelzenberg, M. D.; Turner-Evans, D. B.; Kayes, B. M.; Filler, M. A.; Putnam, M. C.; Lewis, N. S.; Atwater, H. A. Photovoltaic Measurements in Single-Nanowire Silicon Solar Cells. *Nano Lett.* **2008**, *8* (2), 710–714.
- (19) Koren, E.; Rosenwaks, Y.; Allen, J. E.; Hemesath, E. R.; Lauhon, L. J. Nonuniform Doping Distribution along Silicon Nanowires Measured by Kelvin Probe Force Microscopy and Scanning Photocurrent Microscopy. *Appl. Phys. Lett.* **2009**, *95* (9), 092105–092107.
- (20) Allen, J. E.; Perea, D. E.; Hemesath, E. R.; Lauhon, L. J. Nonuniform Nanowire Doping Profiles Revealed by Quantitative Scanning Photocurrent Microscopy. *Adv. Mater.* **2009**, *21* (30), 3067–3072.
- (21) Paul, W.; Pearson, G. L. Pressure Dependence of the Resistivity of Silicon. *Phys. Rev.* **1955**, 98 (6), 1755–1757.
- (22) Bridgman, P. W. The Effect of Pressure on the Electrical Resistance of Certain Semi-Conductors. *Proc. Am. Acad. Arts Sci.* **1951**, 79, 127–148.
- (23) Bradby, J. E.; Williams, J. S.; Swain, M. V. In Situ Electrical Characterization of Phase Transformations in Si During Indentation. *Phys. Rev. B* **2003**, 67 (8), 085205–085209.
- (24) Putnam, M. C.; Turner-Evans, D. B.; Kelzenberg, M. D.; Boettcher, S. W.; Lewis, N. S.; Atwater, H. A. Ten  $\mu$ m Minority-Carrier Diffusion Lengths in Si Wires Synthesized by Cu-Catalyzed Vapor-Liquid-Solid Growth. *Appl. Phys. Lett.* **2009**, *95* (16), 163116–163118.
- (25) Sze, S. M.; Ng, K. K. *Physics of Semiconductor Devices*, 3rd ed.; John Wiley & Sons, Ltd: New York, 2007.
- (26) Card, H. C.; Rhoderic, E. H. Studies of Tunnel MOS Diodes I. Interface Effects in Silicon Schottky Diodes. *J. Phys. D: Appl. Phys.* **1971**, 4 (10), 1589–1601.
- (27) Lo, S. H.; Buchanan, D. A.; Taur, Y.; Wang, W. Quantum-Mechanical Modeling of Electron Tunneling Current from the Inversion Layer of Ultra-Thin-Oxide nMOSFET's. *IEEE Electron Device Lett.* **1997**, *18* (5), 209–211.
- (28) Freund, M. S.; Deore, B. A. Self-Doped Conducting Polymers, 1st ed.; John Wiley & Sons, Ltd: New York, 2007.
- (29) Skotheim, T. A.; Reynolds, J. Handbook of Conducting Polymers, 3rd ed.; CRC Press: Boca Raton, FL, 2007.